PEGylated DOTA-AHA-based Gd(III) chelates – A relaxometric study

André Fontes[a], Shima Karimi[b], Lothar Helm*[b], Paula M. Ferreira[a], João P. André*[a]

[a] Centro de Química, Campus de Gualtar, Universidade do Minho, 4710-057 Braga, Portugal

[b] Institut des Sciences et Ingénierie Chimiques, École Polytechnique Fédérale de Lausanne, CH-1015 Lausanne, Suisse

* Corresponding authors: Tel: +351 253 604 385, e-mail: jandre@quimica.uminho.pt; Tel: +41 21 693 9876; e-mail: lothar.helm@epfl.ch

Keywords: DOTA, PEG, gadolinium, MRI, contrast agents

Abstract

Three PEGylated derivatives of 1,4,7,10-tetraazacyclododecane-1-((6-amino)hexanoic)-4,7,10-triacetic acid) (DOTA-AHA) with different molecular weights were prepared and characterized. Their Gd(III) chelates were studied in aqueous solution using variable-temperature ^{1}H nuclear magnetic relaxation dispersion (NMRD) and ^{17}ONMR spectroscopy in view of the determination of their relaxivity and the parameters that govern it. The relaxivity varied from 5.1 to 6.5 $mM^{-1}.s^{-1}$ (37 ºC and 60 MHz) with the increasing molecular weight of the PEG chain, being slightly higher than that of the parent chelate Gd(DOTA-AHA), due to a small contribution of a slow global rotation of the complexes.

A variable temperature ^{1}H NMR study of several Ln(III) chelates of DOTA-A(PEG_{750})HA allowed the determination of the isomeric *M*/*m* ratio (*M* = square antiprismatic isomer and *m* = twisted square antiprismatic isomer, the latter presenting a much faster water exchange) which for the Gd(III) chelate was estimated in *circa* 1:0.2, very close to that of $[Gd(DOTA)]^{-}$. This explains why the PEGylated Gd(III) chelate has a water rate exchange similar to that of $[Gd(DOTA)]^{-}$. The predominance of the *M* isomer is a consequence of the bulky PEG moiety which does not favor the stabilization of the *m* isomer in sterically crowded systems at the substituent site, contrary to what happens with less packed asymmetrical DOTA-type chelates with substitution in one of the four acetate C(α) atoms.

Introduction

Magnetic resonance imaging (MRI) is one of the most powerful and useful techniques in medicine for soft tissue imaging. Images are generated by spatially encoding the signal coming from the water hydrogen nuclei of the tissues through the application of time-varying, linear magnetic field gradients and pulses of radiofrequencies.[1] The quality of a MRI scan depends on intrinsic properties of the biological tissues such as the density (ρ_H) of the hydrogen nuclei, the blood flow and the hydrogen nuclei relaxation times (T_1 and T_2). In *circa* 40% of MRI scans there is the need of paramagnetic contrast agents (CAs) which shorten the hydrogen nuclei relaxation times of neighboring water molecules, increasing the signal intensity on T_1 weighted images and decreasing it on T_2 weighted images, enhancing thus the contrast between the body tissues.[2] Gd(III) is particularly suitable for the purpose of contrast enhancement in T_1 weighted images, due to its high magnetic moment and long electronic relaxation time, which results in a strong dipolar interaction with the hydrogen nuclei.[3]

The vast majority of the approved CAs are Gd(III) chelates based both on macrocyclic tetraazapolyaminocarboxylate chelators (ex: Dotarem®, Prohance® or Gadovist®) and open-chain polyaminocarboxylate chelators (ex: Magnevist®, Omniscan® or Multihance®). These low molecular weight extracellular fluid CAs rapidly equilibrate between the intravascular and interstitial spaces.[4] This equilibrium decreases the effective concentration of Gd(III) within the blood vessels and distributes gadolinium into the interstitial tissues where it may increase background noise.[5]

The effectiveness of any contrast agent is measured by its relaxivity (r), which is the enhancement of the water protons relaxation rate imposed by a 1 mM concentration of Gd(III) chelate.[6] There are several approaches to increase the relaxivity through the optimization of its molecular parameters. The rotational correlation time (τ_R), water exchange rate (k_{ex}) and electron spin relaxation times (T_e) are the most important parameters ruling relaxivity. Because T_e is mainly dependent on the metal ion it is not easily changeable while the other two parameters can be more or less efficiently optimized.[6] To increase the rotational correlation time of the Gd(III) complexes seems to be the most straightforward choice and this has been achieved through several strategies: formation of multinuclear assemblies, either through covalently bound chelates (multimeric structures,[7] linear polymeric structures,[7d, 8] spherical dendrimers[9]) or

through non-covalently bound chelates (micelles,[10] liposomes[10c, 11]). All these multinuclear assemblies of Gd(III) chelates constitute macromolecular CAs which compared to small molecule CAs, besides an enhanced relaxivity, present extended retention in the blood circulation presenting thus great potential in angiography, cancer imaging, kidney imaging, liver imaging, lymphatic imaging, noninvasive visualization of drug delivery, etc.[12]

The insertion of PEG (polyethylene glycol) units in the chelates or in their multinuclear assemblies has been exploited over the years considering the advantages that PEGylation can offer including prolonged retention time in circulation, increased excretion, decreased accumulation in the organs and increased uptake in tumors. The long-chain amphiphilic PEG moieties are inert and can increase the solubility of complexes in water[13] and prolong circulating half-life of proteins, polymers and small molecules.[14] PEGylation has also been shown to reduce immunogenicity.[15] Due to these properties, the incorporation of PEG moieties onto radiolabeled DOTA-based bioconjugates in order to reduce liver uptake and increase tumor accumulation has been reported over the years.[16]

In the search for new MRI CAs, the insertion of PEG units in gadolinium containing systems has been exploited in different manners, from single chelates[17] to copolymeric[8a, 16b, 18] and dendrimeric chelates.[19] The present work aimed at verifying the influence of the introduction of PEG moieties on the relaxivity of Gd(III) chelates of asymmetrical DOTA-based ligands. For this purpose three derivatives of DOTA-AHA (1,4,7,10-tetraazacyclododecane-1-[(6-amino)hexanoic]-4,7,10-triacetic acid) with grafted PEG chains with distinct molar masses (750, 550 and 350 $g.mol^{-1}$; respectively **L1**, **L2** and **L3** in Figure 1) were synthesized and characterized. The Gd(III) chelates of the three **DOTA-A(PEG)HA** ligands were studied by ^{1}H NMRD and ^{17}ONMR and for a better understanding of the PEG pendant groups influence on the relaxometric properties, ^{1}H NMR studies of several paramagnetic lanthanide chelates of **DOTA-A(PEG$_{750}$)HA** were also conducted.

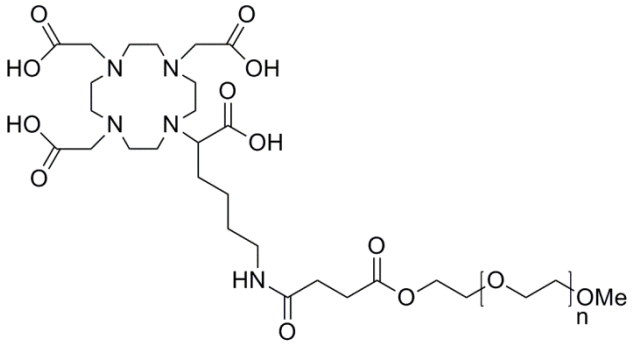

DOTA-A(PEG)HA
n = 16, **L1**
n = 11, **L2**
n = 6, **L3**

Figure 1. DOTA-A(PEG)HA (**L1**, **L2**, **L3**).

Results and Discussion

Synthesis

The PEGylation of DOTA-AHA was accomplished using activated PEG moieties with succinic anhydride (scheme 1, compounds 2-4) with the pro-ligand DOTA-AHA (scheme 1, compound 1). The DOTA-AHA pro-chelator was prepared according to the methodology described recently.[20] After deprotection, the PEGylated ligands 1,4,7,10-tetraazacyclododecane-1-[6-amino(succinate-PEG_{750}-OMe)hexanoic)]-4,7,10-triacetic acid (**L1** = DOTA-A(PEG_{750})HA), 1,4,7,10-tetraazacyclododecane-1-[6-amino(succinate-PEG_{550}-OMe)hexanoic]-4,7,10-triacetic acid (**L2** = DOTA-A(PEG_{550})HA) and 1,4,7,10-tetraazacyclododecane-1-[6-amino(succinate-PEG_{350}-OMe)hexanoic]-4,7,10-triacetic acid (**L3** = DOTA-A(PEG_{350})HA) were isolated in good yields.

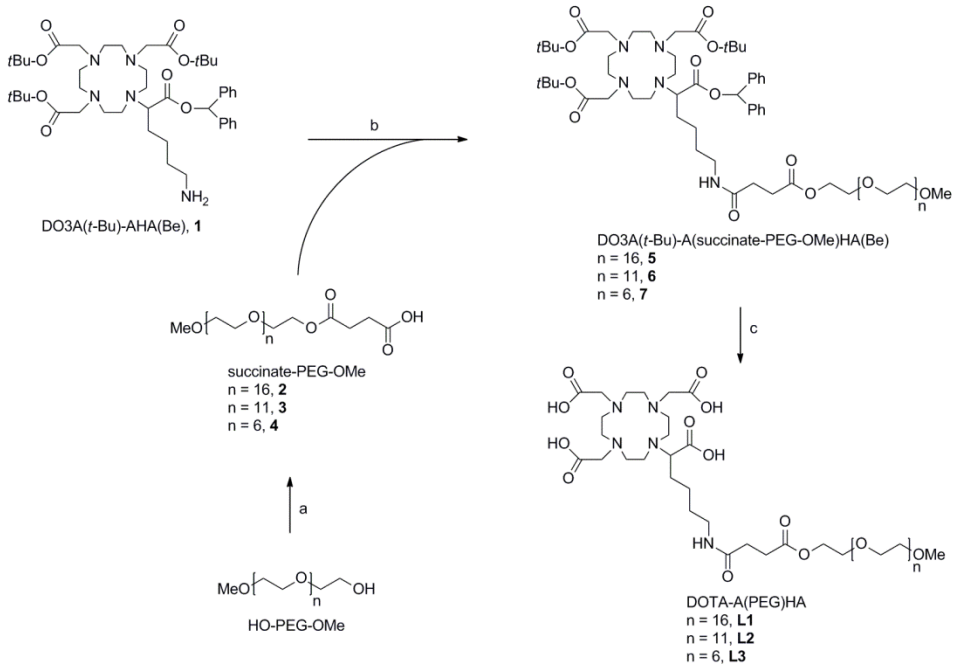

Scheme 1. Synthesis of DOTA-AHA PEGylated conjugates. **A)** succinic anhydride, $CHCl_3$, H_2SO_4 (95%); **b)** DIPEA, HATU, HOBt, MeCN; **c)** TFA, DCM.

^{1}H NMRD and ^{17}O NMR relaxometric studies

To obtain the parameters determining the relaxivity, all PEGylated Gd(III) chelates have been studied by ^{1}H relaxometry (Figure 2) and the chelate **[Gd(L2)]**$^{-}$ has also been studied by ^{17}O NMR relaxation and chemical shifts measurements (Figure 3). The results of a combined analysis using the Solomon-Bloembergen-Morgan model of the latter chelate show that water exchange rate (Table 1) is not influenced by PEGylation in relation to Gd(DOTA), being actually slightly higher than that of this chelate ($^{298}k_{ex} = 4.1\text{x}10^{6}$ s^{-1}).[21] These results are in contrast with what has been previously reported for the PEGylated hetero-tripodal hydroxypyridonate (HOPO) gadolinium complexes, since the coupling of PEG moieties lead to a decrease in the k_{ex} values in relation to HOPO complexes without PEG.[17a, 17c] In this case, the authors ascribed such effect to the formation of hydrogen bonds with water molecules which induce partial displacement of the inner sphere water molecules; the strength of these bonds being strong enough for the reduction of the number of water molecules in the inner sphere (q) from 2 (non-PEGylated chelate) to 1 (PEGylated chelates).[17a, 17c] Fixing a long chain like PEG in the more rigid **[Gd(DOTA-A(PEG)HA)]**$^{-}$ has only a minor influence on its structure (see *M/m* ratio in next section), and consequently no such effect on the water molecule residence time is observed. We therefore fixed the water exchange rate constants in the analysis of the relaxivity data to the values of **[Gd(L2)]**$^{-}$ (Table 1).

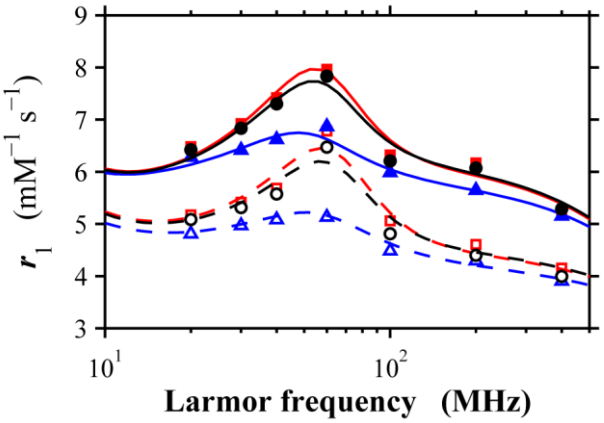

Figure 2. ^{1}H NMRD profile of [**Gd(L1)]**$^-$ (■, □**;** red), [**Gd(L2)]**$^-$ (●, ○**;** black) and [**Gd(L3)]**$^-$ (▲, Δ**;** blue) chelates at 25 ºC (filled symbols) and 37 °C (empty symbols). The lines represent the best fit of the data resulted from simultaneous fitting based on SBM equations.

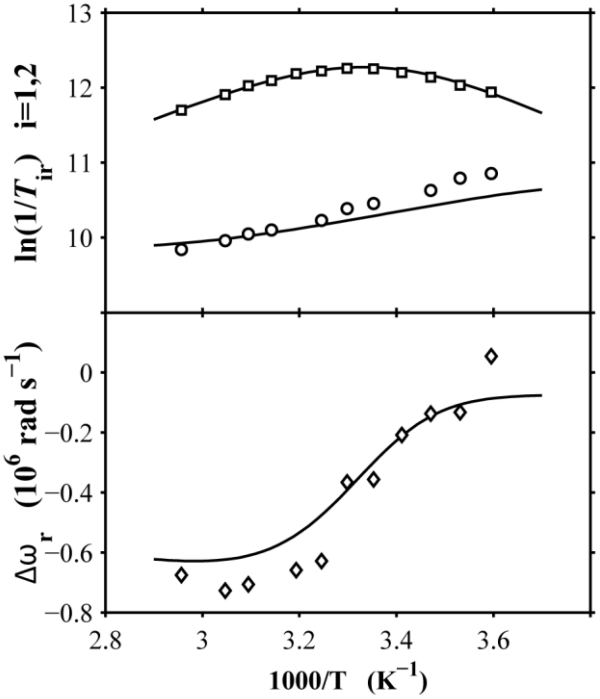

Figure 3. Reduced ^{17}O transverse (□) and longitudinal (○) relaxation rates and reduced chemical shifts (◊) (*B* = 9.4 T) for the **[Gd(L2)]**$^-$ chelate. The lines represent the best simulation fit of experimental data.

The ^{1}H NMRD profiles of the PEGylated compounds (Figure 2) show that the relaxivity reaches its maximum at 60 MHz. PEGylation of the chelates results in improved relaxivity values in relation to its parent chelate Gd(DOTA-AHA)[20] at all applied frequencies (Gd(DOTA-A(PEG$_{750}$)HA): 38% augmentation in r_1 at 37 ºC and 60 MHz). If one compares relaxivity with that of Gd(DOTA) the increase is 110%.[21] This improvement is in contrast to what has been observed on PEGylation of DTPA-BMA based complexes.[8a] This difference can probably be attributed to the 10 times slower water exchange on [Gd(DTPA-BA)-PEG] which is limiting relaxivity in that case.

Table 1. Relaxometric parameters for [**Gd(L1)]**$^{-}$, [**Gd(L2)]**$^{-}$ and [**Gd(L3)]**$^{-}$ The [**Gd(L2)]**$^{-}$ parameters were obtained from the simultaneous analysis of ^{17}O NMR and ^{1}H NMRD data, using the Solomon-Bloembergen-Morgan approach[(a)(b)].

Parameter	[**GdL1]**$^{-}$	[**GdL2]**$^{-}$	[**GdL3]**$^{-}$
$\Delta H^{\ddagger}$ **(kJ.mol^{-1})**	*47*	47 ± 5.4	*47*
$^{298}k_{ex}$ **(10^{6} s^{-1})**	*5.0*	5.1 ± 0.8	*5.0*
A/$\hbar$ (10^{6} rad.s^{-1})		-2.9 ± 0.2[(c)]	
Cos		0.1	
$^{298}\tau_g$ **(ps)**	> 40000	10000	9000 ± 7000
$^{298}\tau_i$ **(ps)**	235 ± 9	231 ± 7	212 ± 4
S^2	0.05 ± 0.01	0.041 ± 0.006	0.02 ± 0.003
$^{298}\tau_v$ **(ps)**	13 ± 3	16 ± 2	22 ± 3

(a) The italicized values of parameters in the table were calculated from ^{17}O NMR measurements of [**Gd(L2)]**$^{-}$ and kept as constant parameters for the NMRD fitting of the other two [**Gd(L1)]**$^{-}$ and [**Gd(L3)]**$^{-}$ compounds.

(b) Other parameters fixed in the fitting procedure are: $\Delta^2/10^{20}$ = 1.0 s^{-2}, r_{GdO} = 2.5 Å, r_{GdH} = 3.1 Å, a_{GdH} = 3.6 Å, E_{GdH} = 20 kJ.mol^{-1} and q = 1.

(c) The unusually small value of A/$\hbar$ is due to experimental ^{17}O $1/T_{2r}$ data and $1/T_{1e}$ which is mainly defined by ^{1}H NMRD.

Through the analysis of the ^{1}H NMRD profiles, it is also noticeable that the relaxivity is related to the PEG molecular weight. **[Gd(L1)]**$^{-}$(r_1 = 6.5 mM^{-1}.s^{-1}at 37 ºC and r_1 = 8.0 mM^{-1}.s^{-1}at 25 ºC and 60 MHz), which is the chelate with an heavier PEG moiety, has higher relaxivity in comparison to **[Gd(L2)]**$^{-}$(r_1 = 5.9 mM^{-1}.s^{-1}at 37 ºC and r_1 = 7.8 mM^{-1}.s^{-1}at 25 ºC and 60 MHz), which in turn has a higher value than that of the smaller chelate **[Gd(L3)]**$^{-}$ (r_1 = 5.1 mM^{-1}.s^{-1}at 37 ºC and r_1 = 6.8 mM^{-1}.s^{-1}at 25 ºC and 60 MHz). This

trend is most perceptible at frequencies where the rotational correlation time has more influence on the relaxivity values (between 40 and 100 MHz).

The NMRD profiles (Figure 2) could only be fitted using a Lipari-Szabo model free approach taking into account internal rotational motion.[22] All three compounds show a very long τ_g corresponding to the global rotation of the complexes and a much shorter τ_l describing the actual rotation of the Gd-H vectors (Table 1).The model free order parameter S^2 is for all compounds very small with values from 0.05 to 0.02. This shows that the rotation of the Gd-H vector is largely dominated by the short local correlation time which is for all compounds between 210 to 235 ps. The global rotation of the ligands with longer PEG chains **[Gd(L1)]**$^-$ and **[Gd(L2)]**$^-$ are slow (10 ns) and even the compound with the shortest PEG chain has a $\tau_g \approx 9$ ns. A consequence of the small values for $S^2$is the small relaxivity hump shown for all three compounds. However, even for such a small order parameter, the contribution of the global motion leads to a relaxivity increase of ≈ 20% at 60 MHz (Figure 4). At high magnetic fields ($B_0 > 3$ T) the slow global motion has no influence on the relaxivities.

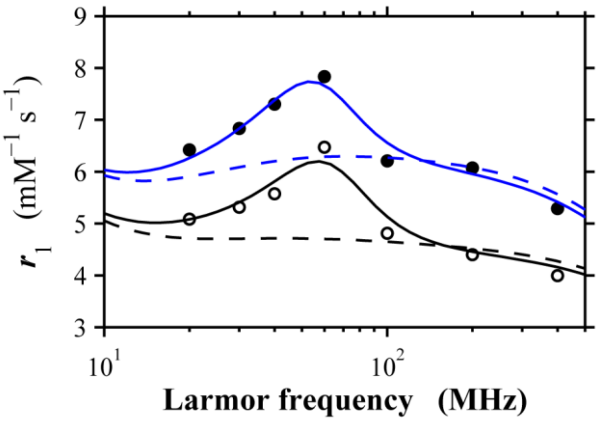

Figure 4. ^{1}H NMRD profile of [**Gd(L2)**]$^-$ at 25 ºC (filled symbols) and 37 °C (empty symbols). The lines represent the best fit of the data (S^2 = 0.04); the dashed lines are calculated using the same parameters except S^2 set to zero.

^{1}H NMR studies of paramagnetic lanthanide L1 chelates

The trivalent lanthanide complexes of DOTA-based ligands exhibit a variety of conformational and coordination isomers which may display dynamic behavior on the NMR timescale.[23] The isomers of their Gd(III) chelates have been found to have different relaxivity properties.[24] Considering this, some ^{1}H NMR studies have been performed with some paramagnetic lanthanide **L1** chelates.

^{1}H NMR is a valuable technique for the solution study of the isomers of the Ln(III) complexes of DOTA and its derivatives.[23a, 23b] The high symmetry of DOTA leads to the existence of two isomers of the $[Ln(DOTA)]^-$ chelates in solution, with square antiprismatic (*M*) and twisted square antiprismatic (*m*) geometries.[25] These isomers have the same [3.3.3.3] square conformation with fourfold symmetry of the tetraazacyclododecane ring, where all its ethylenic groups adopt a δ or λ conformation, thus leading to conformations of clockwise or counterclockwise helicity, λλλλ or δδδδ. They only differ on the layout of the four acetate pendant arms, resulting from rotations around the N-CH_2-CO_2 bonds, with either a clockwise (Λ) or counterclockwise (Δ) helicity. These lead to the two diastereoisomers existing in solution (*m* and *M*), with separate NMR resonances, each of which is an enantiomer pair: the square antiprismatic (*M*) geometry results from the opposite helicity of the tetraaza ring and the acetate arms (Δ(λλλλ) or Λ(δδδδ)), while the twisted antiprismatic (*m*) geometry has the same ring and acetate helicity (Λ(λλλλ) or Δ(δδδδ)). Thus *M* and *m* differ in the value and sign of the twist angle α between the diagonals of the parallel squares formed by four N-atoms and the four carboxylate O-atoms in the coordination polyhedron of the DOTA chelates (typical values of $\alpha \approx +35^o$ and $\alpha \approx -15^o$, respectively, found from crystallographic structures).[23a] The isomer *M* shows a wider paramagnetic shift range than *m* throughout the lanthanide series. The isomer *m* is dominant relative to *M* for the early Ln(III) chelates (Ln = La – Pr), but *M* becomes dominant for the smaller ions (Ln = Eu – Lu).[23c]

Similarly to the ligand DOTASA,[26] **L1** is an asymmetrical derivative of DOTA, with one of the four acetate C(*α*) atoms substituted. In the case of **L1** the asymmetry is introduced through the inclusion of an amide-PEG-bearing group, leading to the existence of a chiral center in the ligand and a site of asymmetry in the complexes which double the number of possible isomeric species. As we have obtained the ligand **L1** as a racemic mixture of the (α*R*) and (α*S*) enantiomers, the complete identification of all possible stereoisomers requires identification of the configuration (α*R*) of the chiral C-atom of the

ligand, together with the four arrangements of the ligand itself in the complex described above for DOTA complexes. Due to this, in solution there can be up to eight stereoisomers of **[Ln(L1)]**$^{-}$ of the type *W*-*X* (*W* = I or (*S*); *X* = *M* (Δ(λλλλ) or Λ(δδδδ)) or *m* (Λ(λλλλ) or Δ(δδδδ)), consistent with four enantiomer pairs: I-*M*, I-*m*, (*S*)-*M* and (*S*)-*m*. Considering this, up to four sets of ^{1}H NMR signals are to be expected from these enantiomer pairs. The lack of C_4 symmetry removes the signal degeneracy found in the NMR spectra of [Ln(DOTA)]$^{-}$ complexes and leads to a large number of resonances for each isomer in the ^{1}H NMR spectra.

The special properties of the paramagnetic Pr(III), Nd(III), Sm(III) and Eu(III) chelates of **L1** were investigated by ^{1}H NMR at three different temperatures (25 ºC, 40 ºC and 60 ºC), showing a large number of partially overlapping resonances covering paramagnetic shift ranges in accordance with those observed for the corresponding DOTA chelates.[25b, 25d] Previous ^{1}H NMR studies with the symmetrical [Ln(DOTA)]$^{-}$ chelates, and with a variety of lanthanide derivatives of DOTA,[23a] have demonstrated that the two diastereoisomers *m* and *M* are present in solution, with a relative proportion that is a function of the lanthanide ion, temperature, solvent and the steric crowding of the chelate.[23a, 23c] Steric crowding favors the *m* isomer and this has been demonstrated by comparing the populations of both isomers of lanthanide(III) complexes of DOTA and DOTA analogs.[27]

The two isomers are characterized by different dipolar shifts, with complexes of the *M* form possessing the larger paramagnetic shift for a given ligand resonance. Through the analysis of the obtained ^{1}H NMR spectra, the *M*/*m* isomer ratio could be determined for several complexes. For this purpose it is particularly useful to observe the resonance in the most-shifted axial ring proton, ax_1, which is well separated from the others.[23a, 23c, 25] For example, in the case of [Ln(DOTA)]$^{-}$ complexes this resonance is observed at *circa* +30-50 ppm and *circa* +150-160 ppm for the *M* isomers, while for the corresponding *m* forms, the axial ring protons ax_1 has resonances at lower frequencies, at *circa* +10-30 ppm and *circa* +90-100 ppm for Eu(III) and Yb (III) complexes, respectively.[23a, 28] Similarly to what has been previously found in asymmetric DOTA-based complexes, the ax_1 protons of most of the studied Ln(III) complexes of **L1** originated two sets of well separated signals, which could be assigned to the isomers *M* and *m*, as shown in Figures 5 and 6. The chemical shifts of the axial protons in the chelates of Pr(III), Nd(III) and Sm(III) are negative while in the case of Eu(III) they are positive, according to the Bleaney constants, which are negative for the first cations and positive for the latter.[29]

Integration of those signals afforded the isomer ratios *M*/*m*, as shown in Table 2. As expected, isomer *m* is dominant for the early lanthanide chelate (praseodymium), decreasing its fraction along the lanthanide series, as the ionic radius of the Ln(III) ions decreases.[23a, 23c] Density functional theory (DFT) calculations on DOTA-like complexes showed that the stabilization of the *M* isomer on proceeding to the right across the lanthanide series is the result of an increased binding energy of the ligand to the metal for this isomer as the charge density of the lanthanide ion increases.[27b]

It is known that *m* isomers of lanthanide macrocyclic DOTA-type chelates have about 50 times faster water exchange (k_{ex}) than *M* isomers.[30] For $[Gd(DOTA)]^-$ an *M*/*m* isomer ratio of *circa* 6:1 was calculated by interpolation of the ratio for the Eu(III) and Tb(III) chelates, while for $[Gd(DOTASA)]^{2-}$ an isomer ratio of 1:1 was obtained, accounting for a 50% increase in the water exchange rate of the latter chelate.[26] The comparison of the observed *M*/*m* ratio for the present PEGylated chelate shows that despite the preservation of the trend in the *M*/*m* ratio just described, the dominance of the *m* isomer for the complexes of the early Ln(III) ions is not so significant as in other cases.[26, 28b] By analogy with the ratio obtained for other Gd(III) chelates, which show to be close to that of the corresponding Eu(III) chelates, a value of *circa* 1:0.2 can be estimated for our Gd(III) chelate, very close to that of $[Gd(DOTA)]^-$. This might be a consequence of the PEG moiety, which is a bulky substituent that does not favor the stabilization of the *m* form in sterically crowded systems [28c] as it happens in less bulky systems, such as in DOTASA chelates.[31] The predominance of the *M* isomer could explain why **$[Gd(L1)]^-$** has a similar water exchange rate to $[Gd(DOTA)]^-$. Exchange between the *m* and *M* isomers is demonstrated by the broadening at 40 ºC (Figure 6) and further signal collapse of the resonances of both isomers observed at 60 ºC.[25c]

Table 2. ^{1}H NMR chemical shifts (ppm) of the ax_1 protons of the paramagnetic lanthanide **L1** chelates in *M* and *m* isomeric forms at 25 °C and pH=7.

Metal Ion	*M* Isomer	*m* Isomer	*M*/*m* Ratio
Pr	-47.16; -40.31	-31.55; -28.81; -24.81; -23.87	1 : 1.5
Nd	-24.38; -21.21	-11.99; -10.31; -8.24; -7.80	1 : 1
Sm	-3.53; -3.04; -2.49	Not Assigned	---
Eu	33.16; 36.83	13.34; 14.01; 16.77; 18.19	1 : 0.25

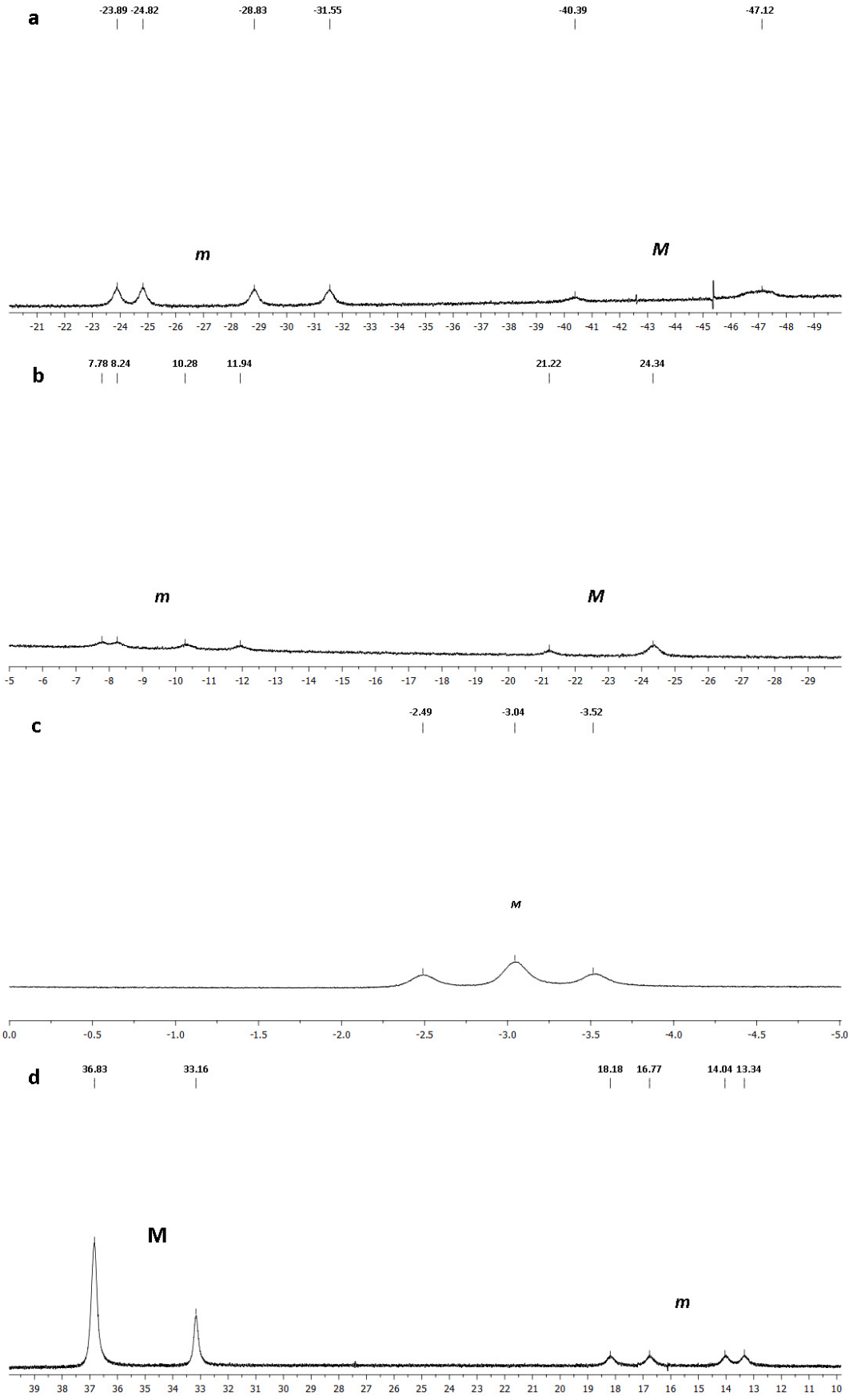

Figure 5. ^{1}H NMR resonances of the ax_1 protons of the *M* and *m* isomers of the paramagnetic lanthanide **L1** chelates at pH=7.1 and 25 °C. **a)** Ln = Pr; **b)** Ln = Nd; **c)** Ln = Sm; **d)** Ln = Eu.

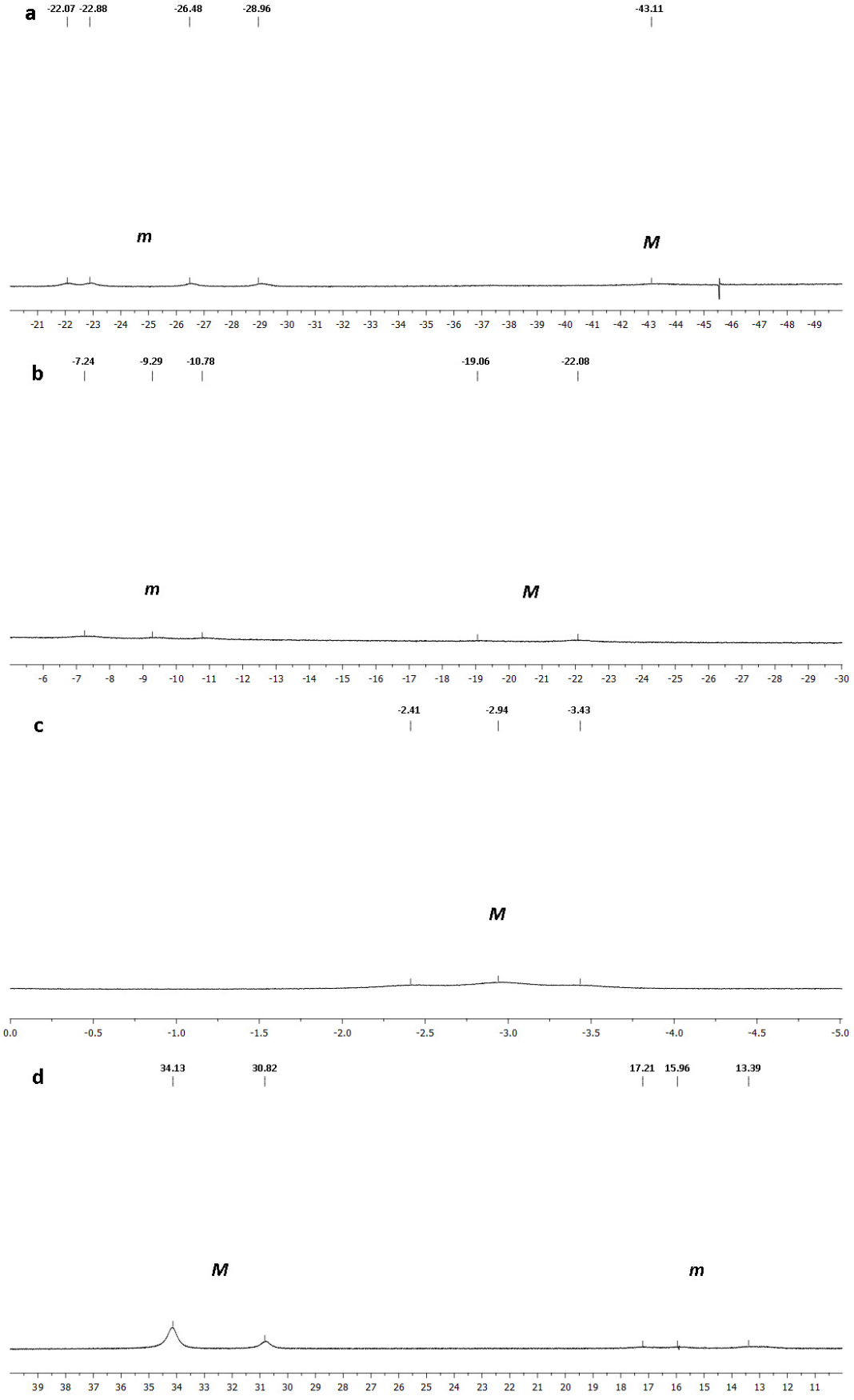

Figure 6. ^{1}H NMR resonances of the ax_1 protons of the *M* and *m* isomers of the paramagnetic lanthanide **L1** chelates at pH=7.1 and 40 °C. **a)** Ln = Pr; **b)** Ln = Nd; **c)** Ln = Sm; **d)** Ln = Eu.

Conclusion

Using a synthetic methodology previously described for the chelator DOTA-AHA, it was possible to prepare three PEGylated derivatives [DOTA-A(PEG)HA]. The Gd(III) chelates of these ligands were designed as potential MRI contrast agents, taking into consideration an enhancement of the relaxivity thanks to longer rotational correlation times and the fact that PEG moieties may also act as pharmacokinetic modifiers, including a prolongation of their circulating time, with concomitant possibility of using them in angiography.

The three PEGylated Gd(III) chelates were studied by ^{1}H relaxometry and ^{17}O NMR was used for the characterization of **[Gd(L2)]**$^{-}$, allowing the determination of the parameters that govern their relaxivities.The PEGylation of Gd(DOTA-AHA) resulted in a relaxivity increase, which is specially noteworthy considering that in the past other authors have considered the PEGylation of paramagnetic chelates a not so efficient way of increasing relaxivity. Our results can be explained taking into consideration that a) PEGylation did not decrease the number of bound water molecules; b) PEGylation did not affect negatively the water exchange rate; c) the rotational motion is dominated by fast local motion with a small contribution due to a slow global reorientation.

^{1}H NMR studies of paramagnetic **[Ln(L1)]**$^{-}$ chelates were conducted, putting in evidence the ratio of the square antiprismatic (*M*) and the twisted square antiprismatic isomers (*m*) in solution. Contrary to other DOTA-type chelates asymmetrically substituted in one of the four acetate C(α) atoms, which in some cases can increase the proportion of the *m* isomer which displays the faster water exchange rate, the inclusion of PEG chains in the chelates did not alter the isomeric *M*/*m* ratio proportion, which in this regard is similar to that of [Gd(DOTA)]$^{-}$.

Experimental

Chemicals and Materials

Analytical grade solvents were used and dried by the usual methods when was needed. Analytical grade reagents were purchased from Sigma-Aldrich, Acros, Bachem, Merck, Chematech and used without further purification. ^{17}O-enriched water was purchased from IsoTrade GmbH (Mönchengladbach, Germany).

The reactions were monitored by thin layer chromatography (TLC) on glass plates coated with silica gel 60 F_{254} (Whatman) and detection was made by examination under UV light (240 nm), by adsorption of iodine vapor and/or by spraying with ninhydrin. Chromatographic separations were performed on silica gel 60 (Whatman 230-240 Mesh).

Instruments

The ^{1}H and ^{13}C NMR spectra (assigned by DEPT, HSQC and HMBC techniques) were recorded on a Bruker Avance III 400 spectrometer, operating at 400.13 MHz and 100.62 MHz, for ^{1}H and ^{13}C NMR respectively. The ^{1}H NMR spectra of DOTA-A(PEG_{750})HA paramagnetic lanthanide complexes were recorded on a Varian Unity Plus 300, operating at 299.938 MHz. The chemical shifts (δ) are reported in ppm, relative to TMS (tetramethylsilane) for $CDCl_3$ solvent (^{1}H, δ=7.26; ^{13}C, δ=77.16) or DMSO solvent (^{1}H, δ=2.50; ^{13}C, δ=39.52), and relative to TSP (3-(trimethylsilyl)propionic-2,2,3,3-d_4 acid sodium salt) for D_2O solvent (^{1}H, δ=4.79).[32] The pH measurements were performed on a pH meter Crimson micro TT 2050 with an electrode Mettler Toledo InLab 422.

The proton longitudinal relaxation rates ($1/T_1$) for the water nuclear magnetic relaxation dispersion profiles (NMRD) were measured using the following equipment: Bruker minispecs mq20 0.47 T (^{1}H Larmor frequency: 20 MHz); mq30 0.70 T (30 MHz); mq40 0.94 T (40 MHz); and mq60 1.41 T (60 MHz); Bruker Avance console connected to 2.35 T (100 MHz) and 4.7 T (200 MHz) cryomagnets and Bruker Avance II 9.4 T (400 MHz). The temperature was controlled either by a thermostated gas flow (cryomagnets) or by pumping a thermostated liquid trough the probe (minispecs). All temperatures were measured by substitution technique.[33] The variable-temperature ^{17}O measurements were performed on a Bruker Avance II 9.4 T (^{17}O Larmor frequency:

54.3 MHz) spectrometer, equipped with a Bruker BVT3000 temperature control unit and a Bruker BCU05 cooling unit. The susceptibility measurements were performed on a Bruker Avance 400 spectrometer, also equipped with a BVT-3000 temperature control unit.

Synthesis

succinate-PEG$_{750}$-OMe, 2

HO-PEG$_{750}$-OMe (4.2 g, 5.4 mmol) was dissolved in dry $CHCl_3$ (20 mL) and to this solution succinic anhydride (554 mg, 5.3 mmol) and a catalytic amount of sulfuric acid (95%) were added. The solution was stirred for 6 hours at reflux temperature and concentrated under reduced pressure to afford compound **2** (4.7 g) as a colorless oil. The product was used without further purification. ^{1}H NMR (400 MHz, $CDCl_3$, TMS) δ: 2.61-2.71 (4H, m, α- and β-CH_2 succinate), 3.38 (3H, s, OMe), 3.54-3.56 (2H, m, O-CH_2 PEG), 3.59-3.72 (nH, m, β-CH_2 PEG + nPEG), 4.24-4.27 (2H, m, α-CH_2 PEG) ppm. ^{13}C NMR (100 MHz, $CDCl_3$, TMS) δ: 28.95 (α-CH_2 succinate), 29.41 (β-CH_2 succinate), 58.98 (OMe), 63.80 (α-CH_2 PEG), 68.93 (β-CH_2 PEG), 70.46, 70.48, 70.50 (nPEG), 71.88 (O-CH_2 PEG), 172.02 (C=O), 174.36 (C=O) ppm. LRMS (ESI$^+$) – m/z: calculated for: n = 17 – $C_{41}H_{80}O_{22}$ (MH^+) 925.52; found 925.75 (MH^+); n = 16 – $C_{39}H_{76}O_{21}$ (MH^+) 881.50; found 881.75, (MH^+); n = 15 – $C_{37}H_{72}O_{20}$ (MH^+) 837.47; found 837.67, (MH^+); n = 14 – $C_{35}H_{68}O_{19}$ (MH^+) 793.44; found 793.69, (MH^+); n = 13 – $C_{33}H_{64}O_{18}$ (MH^+) 749.42; found 749.70 (MH^+).

succinate-PEG$_{550}$-OMe, 3

Using a similar procedure to that previously described for compound **2**, but using HO-PEG$_{550}$-OMe (2.2 g, 3.7 mmol) it was possible to obtain compound **3** (2.5 g) as a colorless oil. The product was used without further purification.^{1}H NMR (400 MHz, DMSO, TMS) δ: 2.43-2.58 (4H, m, α- and β-CH_2 succinate), 3.23 (3H, s, OMe), 3.39-3.43 (2H, m, O-CH_2 PEG), 3.46-3.54 (nH, m, nPEG), 3.58 (2H, t, *J*=4.8 Hz, β-CH_2 PEG), 4.11 (2H, t, *J*=4.6 Hz, α-CH_2 PEG) ppm. ^{13}C NMR (100 MHz, DMSO, TMS) δ: 28.61, 28.64 (α- and β-CH_2 succinate), 58.03 (OMe), 63.44 (α-CH_2 PEG), 68.22 (β-CH_2 PEG), 69.57, 69.72, 69.77 (nPEG), 71.27 (O-CH_2 PEG), 171.94 (C=O), 173.35 (C=O) ppm. LRMS (ESI$^+$) – m/z: calculated for: n = 13 – $C_{33}H_{64}O_{18}$ (MH^+) 749.42; found 749.83, (MH^+); n = 12 – $C_{31}H_{60}O_{17}$ (MH^+) 705.39; found 705.50, (MH^+); n = 11 – $C_{29}H_{56}O_{16}$ (MH^+) 661.36;

found 661.42, (MH^+); n = 10 – $C_{27}H_{52}O_{15}$ (MH^+) 617.34; found 317.42, (MH^+); n = 9 – $C_{25}H_{48}O_{14}$ (MH^+) 573.31; found 573.52 (MH^+).

succinate-PEG$_{350}$-OMe, 4

Using a similar procedure to that previously described for compound **2**, but using HO-PEG$_{350}$-OMe (4.3 g, 12.2 mmol) it was possible to obtain compound **4** (5.4 g) as a colorless oil. The product was used without further purification. ^{1}H NMR (400 MHz, DMSO, TMS) δ: 2.43-2.59 (4H, m, α-CH_2 succinate + β-CH_2 succinate), 3.23 (3H, s, OMe), 3.39-3.44 (2H, m, o-CH_2 PEG), 3.48-3.55 (nH, m, nPEG), 3.59 (2H, t, *J*=4.8 Hz, β-CH_2 PEG), 4.11 (2H, t, *J*=4.6 Hz, α-CH_2 PEG) ppm. ^{13}C NMR (100 MHz, DMSO, TMS) δ: 28.57, 28.64 (α-CH_2 succinate) + (β-CH_2 succinate), 58.02 (OMe), 63.44 (α-CH_2 PEG), 68.23 (β-CH_2 PEG), 69.56, 69.72, 69.77 (nPEG), 71.27 (o-CH_2 PEG), 171.89 (C=O), 173.34 (C=O) ppm. LRMS (ESI^+): calculated for: n = 9 – $C_{25}H_{48}O_{14}$ (MH^+) 573.31; found 573.70 (MH^+); n = 8 – $C_{23}H_{44}O_{13}$ (MH^+) 529.29; found 529.36 (MH^+); n = 7 – $C_{21}H_{40}O_{12}$ (MH^+) 485.26; found 485.63 (MH^+); n = 6 – $C_{19}H_{36}O_{11}$ (MH^+) 441.23; found 441.92 (MH^+); n = 5 – $C_{17}H_{32}O_{10}$ (MH^+) 397.21; found 397.83 (MH^+).

DO3A(*t*-Bu)-A(succinate-PEG$_{750}$-OMe)HA(Be), 5

DO3A(*t*-Bu)-AHA(Be) (370 mg, 457 μmol) was dissolved in dry MeCN (30 mL) and to this solution, succinate-PEG$_{750}$-OMe (544 mg, 640 μmol), DIPEA (80 μL, 457 μmol), HOBt (104 mg, 767 μmol) and HATU (292 mg, 767 μmol) were added. The solution was stirred for 48 hours at room temperature and more HOBt (104 mg, 767 μmol) and HATU (292 mg, 767 μmol) were added. The solution was stirred for more 48 hours at room temperature and concentrated under reduced pressure to give a yellow oil. The oil was dissolved in ethyl acetate (75 mL), and the organic phase was washed with $KHSO_4$ 1M (2 x 45 mL), $NaHCO_3$ 1M (2 x 45 mL) and brine (2 x 45 mL). The organic phases were combined, dried with anhydrous $MgSO_4$ and concentrated under reduced pressure to afford compound **5** (485 mg, 65 %) as a yellow solid. ^{1}H NMR (400 MHz, $CDCl_3$, TMS) δ: 1.15-1.50 (31H, m_b, γ-CH_2 + δ-CH_2 + CH_3*t*-Bu), 1.62-1.81 (2H, m, β-CH_2), 1.97-3.34 (28H, m, CH_2 cyclen + ε-CH_2 + CH_2COR + α-CH_2 succinate + β-CH_2 succinate), 3.36 (3H, s, OMe), 3.50-3.65 (nH, m_b, nPEG + α-CH), 3.65-3.73 (2H, m, β-CH_2 PEG), 4.13-4.22 (2H, m, α-CH_2 PEG), 6.86 (1H, s, CH Benzhydryl), 7.20-7.44 (10H, m, ArH) ppm. ^{13}C NMR (100 MHz, $CDCl_3$, TMS) δ: 26.43 (γ-CH_2), 27.78 (CH_3*t*-Bu), 28.91, 29.33, 29.60 (β-CH_2 + δ-CH_2 + α-CH_2 succinate), 30.62 (β-CH_2 succinate), 39.00 (ε-CH_2),

44.38, 47.36, 47.80, 48.15 (CH_2 cyclen), 55.53 (*C*H_2COR), 58.83 (OMe), 61.35 (α-CH), 63.46 (α-CH_2 PEG), 68.68 (β-CH_2 PEG), 70.13, 70.27, 70.37 (nPEG), 71.69 (o-CH_2 PEG), 78.09 (CH Benzhydryl), 81.91 (C *t*-Bu), 126.41 (ArH), 128.15 (ArH), 128.54 (ArH), 139.98 (C ArH), 171.65 (C=O), 172.12 (C=O), 172.54 (C=O *t*-Bu), 175.10 (C=O Benzhydryl) ppm.

DO3A(*t*-Bu)-A(succinate-PEG$_{550}$-OMe)HA(Be), 6

Using a similar procedure to the previously described for compound **5**, but with succinate-PEG$_{550}$-OMe (324 mg, 498 μmol) it was possible to obtain compound **6** (347 mg, 68 %) as a yellow solid. ^{1}H NMR (400 MHz, $CDCl_3$, TMS) δ: 1.18-1.57 (31H, m_b, γ-CH_2 + δ-CH_2 + CH_3 *t*-Bu), 1.61-1.79 (2H, m, β-CH_2), 1.97-3.31 (28H, m_b, CH_2 cyclen + ε-CH_2 + CH_2COR + α-CH_2 succinate + β-CH_2 succinate), 3.34 (3H, s, OMe), 3.49-3.65 (nH, m, nPEG + α-CH), 3.66-3.69 (2H, m, β-CH_2 PEG), 4.17-4.24 (2H, m, α-CH_2 PEG), 6.86 (1H, s, CH Benzhydryl), 7.22-7.39 (10H, m, ArH) ppm. ^{13}C NMR (100 MHz, $CDCl_3$, TMS) δ: 26.39 (γ-CH_2), 27.77 (CH_3*t*-Bu), 28.90, 29.07, 29.63 (β-CH_2 + δ-CH_2 + α-CH_2 succinate), 30.62 (β-CH_2 succinate), 39.00 (ε-CH_2), 44.29, 47.27, 47.75, 48.10 (CH_2 cyclen), 55.39 (*C*H_2COR), 58.68 (OMe), 61.31 (α-CH), 63.59 (α-CH_2 PEG), 68.88 (β-CH_2 PEG), 69.71, 69.92, 70.19 (nPEG), 71.37 (o-CH_2 PEG), 78.06 (CH Benzhydryl), 81.92 (C *t*-Bu), 126.38 (CH), 128.11 (CH), 128.55 (CH), 140.01 (C ArH), 171.71 (C=O), 172.20 (C=O), 172.84 (C=O *t*-Bu), 175.11 (C=O Benzhydryl) ppm.

DO3A(*t*-Bu)-A(succinate-PEG$_{350}$-Ome)HA(Be), 7

Using a similar procedure to the previously described for compound **5**, but with succinate-PEG$_{350}$-OMe (178 mg, 396 μmol) it was possible to obtain compound **7** (194 mg, 79 %) as a yellow solid. ^{1}H NMR (400 MHz, $CDCl_3$, TMS) δ: 1.18-1.55 (31H, m_b, γ-CH_2 + δ-CH_2 + CH_3*t*-Bu), 1.64-1.82 (2H, m, β-CH_2), 1.96-3.32 (28H, m_b, CH_2 cyclen + ε-CH_2 + CH_2COR + α-CH_2 succinate + β-CH_2 succinate), 3.35 (3H, s, OMe), 3.51-3.65 (nH, m, nPEG + α-CH), 3.65-3.71 (2H, m, β-CH_2 PEG), 4.16-4.25 (2H, m, α-CH_2 PEG), 6.85 (1H, s, CH Benzhydryl), 7.22-7.43 (10H, m, ArH) ppm. ^{13}C NMR (100 MHz, $CDCl_3$, TMS) δ: 26.45 (γ-CH_2), 27.77 (CH_3*t*-Bu), 28.95, 29.34, 29.62 (β-CH_2 + δ-CH_2 + α-CH_2 succinate), 30.60 (β-CH_2 succinate), 38.99 (ε-CH_2), 44.30, 47.28, 47.75, 48.13 (CH_2 cyclen), 55.52 (*C*H_2COR), 58.83 (OMe), 61.30 (α-CH), 63.45 (α-CH_2 PEG), 68.68 (β-

CH_2 PEG), 70.09, 70.26, 70.35 (nPEG), 71.68 (o-CH_2 PEG), 78.06 (CH Benzhydryl), 81.90 (C *t*-Bu), 126.39 (CH), 128.12 (CH), 128.55 (CH), 139.96 (C ArH), 171.65 (C=O), 172.11 (C=O), 172.56 (C=O *t*-Bu), 175.08 (C=O Benzhydryl) ppm.

DOTA-A(PEG$_{750}$)HA, L1

DO3A(*t*-Bu)-A(succinate-PEG$_{750}$-OMe)HA(Be), **5** (480 mg, 292 μmol) was dissolved in DCM (7 mL) and in TFA (7 mL). The solution was stirred overnight at room temperature and concentrated under reduced pressure to give a purple oil. The oil was washed with *n*-hexane (2x) and with water (2x) to give a yellow oil. The oil was dissolved in water (70 mL) and the aqueous solution was washed with DCM (4 x 35 mL) and concentrated under reduced pressure to afford compound **L1** (400 mg) as a yellow solid in a trifluoroacetate salt form. ^{1}H NMR (400 MHz, D_2O, TSP) δ: 1.35-1.93 (6H, m_b, β-CH_2 + γ-CH_2 + δ-CH_2), 2.50-2.59 (2H, m, β-CH_2 succinate), 2.67-2.73 (2H, m, α-CH_2 succinate), 2.88-4.23 (25H, m_b, CH_2 cyclen + α-CH + ε-CH_2 + C*H*$_2$CO$_2$H), 3.39 (3H, s, OMe), 3.51-3.73 (nH, m_b, nPEG), 3.77-3.81 (2H, m, β-CH_2 PEG), 4.25-4.29 (2H, m, α-CH_2 PEG) ppm. ^{13}C NMR (100 MHz, D_2O, TSP) δ: 23.63 (γ-CH_2), 28.00 (β-CH_2), 28.17 (δ-CH_2), 29.43 (α-CH_2 succinate), 30.27 (β-CH_2 succinate), 38.71 (ε-CH_2), 50.47, 51.19, 53.46, 54.35 (CH_2 cyclen), 58.63 (OMe), 60.35 (*C*H_2CO$_2$H),61.17 (α-CH), 64.01 (α-CH_2 PEG), 68.42 (β-CH_2 PEG), 68.42, 69.56, 69.62 (nPEG), 70.97 (o-CH_2 PEG), 168.49 (C=O), 174.41 (C=O), 174.70 (C=O), 176.79 (C=O) ppm. LRMS (ESI$^+$): calculated for: n = 18 – $C_{63}H_{119}N_5O_{30}$ (MH^+) 1426.80, (MH_2^{2+}) 713.90; found 1426.80, (MH^+), 713.87 (MH_2^{2+}); n = 17 – $C_{61}H_{115}N_5O_{29}$ (MH^+) 1382.78, (MH_2^{2+}) 691.89; found 1382.78, (MH^+), 691.86 (MH_2^{2+}); n = 16 – $C_{59}H_{111}N_5O_{28}$ (MH^+) 1338.75, (MH_2^{2+}) 669.88; found 1338.75, (MH^+), 669.85 (MH_2^{2+}); n = 15 – $C_{57}H_{107}N_5O_{27}$ (MH^+) 1294.72, (MH_2^{2+}) 647.86; found 1294.72, (MH^+), 647.83 (MH_2^{2+}); n = 14 – $C_{55}H_{103}N_5O_{26}$ (MH^+) 1250.70, (MH_2^{2+}) 625.85; found 1250.70, (MH^+), 625.82 (MH_2^{2+}).

DOTA-A(PEG$_{550}$)HA, L2

Using a similar procedure to the previously described for compound **L1**, but using DO3A(*t*-Bu)-A(succinate-PEG$_{550}$-OMe)HA(Be) (347 mg, 241 μmol) it was possible to obtain compound **L2** (313 mg) as a yellow solid in trifluoroacetate salt form. ^{1}H NMR (400 MHz, D_2O, TSP) δ: 1.31-1.86 (6H, m_b, β-CH_2 + γ-CH_2 + δ-CH_2), 2.43 (2H, t, J=6.6Hz, β-CH_2 succinate), 2.56 (2H, t, *J*=6.4Hz, α-CH_2 succinate), 2.72-4.25 (25H, m_b,

CH_2 cyclen) + α-CH + ε-CH_2 + C*H*$_2$$CO_2$H), 3.28 (3H, s, OMe), 3.50-3.70 (nH, m_b, nPEG + β-CH_2 PEG), 4.12-4.17 (2H, m, α-CH_2 PEG) ppm. ^{13}C NMR (100 MHz, D_2O, TSP)δ: 23.64 (γ-CH_2), 28.08 (β-CH_2), 28.65 (δ-CH_2), 29.32 (α-CH_2 succinate), 30.24 (β-CH_2 succinate), 38.89 (ε-CH_2), 45.48, 50.65, 53.19, 54.05 (CH_2 cyclen), 57.96 (OMe), 60.29 (*C*H_2CO_2H),61.07 (α-CH), 63.94 (α-CH_2 PEG), 68.34 (β-CH_2 PEG), 69.32, 69.34, 69.56 (nPEG), 70.89 (o-CH_2 PEG), 168.72 (C=O), 174.36 (C=O), 174.54 (C=O), 176.79 (C=O) ppm. LRMS (ESI^+): calculated for: n = 14 – $C_{55}H_{103}N_5O_{26}$ (MNa^+) 1272.78, ($MNaH^{2+}$) 636.84; found 1272.79, (MNa^+), 638.89 ($MnaH^{2+}$); n = 13 – $C_{53}H_{99}N_5O_{25}$ (MNa^+) 1228.65, ($MNaH^{2+}$) 614.83; found 1382.76, (MNa^+), 614.88 ($MNaH^{2+}$); n = 12 – $C_{51}H_{95}N_5O_{24}$ (MNa^+) 1184.63, ($MNaH^{2+}$) 592.81; found 1184.73, (MNa^+), 592.87 ($MnaH^{2+}$); n = 11 – $C_{49}H_{91}N_5O_{23}$ (MNa^+) 1140.60, ($MnaH^{2+}$) 570.80; found 1140.71, (MNa^+), 570.85 ($MnaH^{2+}$).

DOTA-A(PEG$_{350}$)HA, L3

Using a similar procedure to the previously described for compound **L1**, but using DO3A(*t*-Bu)-A(succinate-PEG$_{350}$-OMe)HA(Be)(277 mg, 223 μmol) it was possible to obtain compound **L3** (252 mg) as a yellow solid in trifluoroacetate salt form. ^{1}H NMR (400 MHz, D_2O, TSP) δ: 1.29-1.83 (6H, m_b, β-CH_2 + γ-CH_2 + δ-CH_2), 2.37-2.47 (2H, m, β-CH_2 succinate), 2.48-2.62 (2H, m, α-CH_2 succinate), 2.75-4.12 (25H, m_b, CH_2 cyclen + α-CH + ε-CH_2 + C*H*$_2$$CO_2$H), 3.34 (3H, s, OMe), 3.46-3.63 (nH, m_b, nPEG), 3.63-3.67 (2H, m, β-CH_2 PEG), 4.10-4.14 (2H, m, α-CH_2 PEG) ppm. ^{13}C NMR (100 MHz, D_2O, TSP) δ: 23.66 (γ-CH_2), 28.06 (β-CH_2), 29.30 (δ-CH_2), 29.37 (α-CH_2 succinate), 30.22 (β-CH_2 succinate), 38.62 (ε-CH_2), 45.36, 50.71, 53.25, 53.95 (CH_2 cyclen), 57.93 (OMe), 60.26 (*C*H_2CO_2H),61.08 (α-CH), 63.92 (α-CH_2 PEG), 68.30 (β-CH_2 PEG), 69.29, 69.31, 69.45 (nPEG), 70.86 (o-CH_2PEG), 168.35 (C=O), 174.47 (C=O), 174.64 (C=O), 176.73 (C=O) ppm. LRMS (ESI^+): calculated for: n = 10 – $C_{47}H_{87}N_5O_{22}$ (MH_2^{2+}) 537.80; found 537.56, (MH_2^{2+}); n = 9 – $C_{45}H_{83}N_5O_{21}$ (MH_2^{2+}) 515.78; found 515.34, (MH_2^{2+}); n = 8 – $C_{43}H_{79}N_5O_{20}$ (MH_2^{2+}) 493.77; found 493.28, (MH_2^{2+}); n = 7 – $C_{41}H_{75}N_5O_{19}$ (MH_2^{2+}) 471.76; found 471.30 (MH_2^{2+}); n = 6 – $C_{39}H_{71}N_5O_{18}$ (MH_2^{2+}) 449.75; found 449.25 (MH_2^{2+}).

Relaxometric Studies

Sample Preparation

To an aqueous solution of the ligand, a $GdCl_3$ solution in a 1:1 mole ratio was added dropwise (a slight excess of ligand was used). The pH was adjusted to around 4 with the addition of a 0.01 M NaOH solution and the solution was stirred for 1 hour at 60 ºC. The pH was adjusted to 5 with the addition of a 0.01 M NaOH solution and the solution was stirred overnight. The pH was then adjusted to 5.7 and the solution was concentrated under reduced pressure.

In all cases, to the final solution, $H_2{}^{17}O$ (^{17}O = 20.2 %) was added to obtain a final 2% ^{17}O-enrichment in order to improve the sensitivity of ^{17}O NMR measurements. The absence of free metal was checked with xylenol orange.[34] The final concentration of Gd(III) was determined by susceptibility measurements in the presence of *t*-butanol.[35] The Gd(III) concentration in the samples were ≈ 8 mM.

^{1}H NMRD

Sample tubes with an outer diameter of 5 mm were used for measurements. The proton longitudinal relaxation rates ($1/T_1$) for the water nuclear magnetic relaxation dispersion profiles (NMRD) were measured at 0.47 T (^{1}H Larmor frequency: 20 MHz), 0.70 T (30 MHz), 0.94 T (40 MHz), 1.41 T (60 MHz), 2.35 T (100 MHz), 4.7 T (200 MHz) and 9.4 T (400 MHz). The longitudinal relaxation rates of three chelates with known concentration were measured at two different temperatures (25 and 37 ºC). Acidified water (pH = 3.0) was used as an external reference. The relaxivities r_1 ($mM^{-1}.s^{-1}$) were calculated using equation 1 using diamagnetic relaxation contributions $1/T_{1(d)}$ of 0.31 s^{-1} (400 MHz) / 0.40 s^{-1} (20 MHz) for 25 ºC and 0.25 s^{-1} (400 MHz) / 0.29 s^{-1} (20 MHz) for 37 ºC, respectively.

$$r_1 = \frac{1}{[Gd(III)]}\left(\frac{1}{T_1} - \frac{1}{T_{1(\mathrm{d})}}\right), \text{with [Gd(III)] in mM} \qquad \textbf{(1)}$$

For full equations see Supplementary Information (SI).

^{17}O NMR

The samples were sealed in glass spheres adapted for 10 mm NMR tubes, in order to avoid susceptibility corrections to the chemical shifts.[36] Variable-temperature ^{17}O measurements were performed at 9.4 T (^{17}O Larmor frequency: 54.3 MHz). The longitudinal ($1/T_1$) and transverse ($1/T_2$) relaxation rates were measured using the inversion-recovery[37] and the Carr–Purcell–Meiboom–Gill[38] pulse sequences, respectively, and chemical shifts ($\Delta\omega$) were measured at 12 different temperatures in the range from 5 to 65 °C. The reduced relaxation rates T_{1r} and T_{2r} and the reduced chemical shift differences $\Delta\omega_r$, with respect to a pH 3.0 water reference (2% ^{17}O-enrichment), were calculated using equations 2 to 4. The number of water molecules in the inner sphere of the complex q was fixed to one.

$$\frac{1}{T_{\mathrm{ir}}} = \frac{1}{P_M}\left(\frac{1}{T_{\mathrm{i}}} - \frac{1}{T_{\mathrm{i}}^{\mathrm{ref}}}\right), \text{where i} = 1, 2 \quad \textbf{(2)}$$

$$\Delta\omega_r = \frac{1}{P_M}\left(\omega - \omega^{\mathrm{ref}}\right) \quad \textbf{(3)}$$

$$P_{\mathrm{M}} = \frac{q[\mathrm{M(n)}]}{55.56} \quad \textbf{(4)}$$

For full equations see Supplementary Information (SI)

Data Analysis

For fits of the ^{1}H NMRD and ^{17}O NMR data, a Solomon–Bloembergen-based theory was used[36b, 39] supplemented with the Lipari–Szabo free-model approach for the internal rotation.[40] The simultaneous fits were performed using Visualiseur/Optimiseur[41] running on a MATLAB® 8.0 (R2012b) platform.

^{1}H NMR studies of paramagnetic lanthanide DOTA-A(PEG$_{750}$)HA chelates

Samples preparation

To an aqueous solution of the ligand, the corresponding $LnCl_3$ solution in 1:1 mole ratio was added dropwise (a slight excess of ligand was used: 5%). The pH was adjusted to around 4 with the addition of a 0.01 M NaOH solution and the solution was stirred for 1 hour at 60 ºC. The pH was adjusted to 5 with the addition of a 0.01 M NaOH solution and the solution was stirred overnight. The pH was then adjusted to 7 and the solution was concentrated under reduced pressure.

Measurements

The solutions were prepared by dissolving the respective chelate in D_2O (700 μL). The proton spectra of the Pr(III), Nd(III), Sm(III), Eu(III) and Yb(III) chelates were obtained at 7, 25, 40 and 60 ºC. The ^{1}H NMR spectra were recorded on a Varian Unity Plus 300 spectrometer, operating at 299.938 MHz.

Abbreviations

Be	Benzhydryl
CA	Contrast agent
Cyclen	1,4,7,10-tetraazacyclododecane
DCM	Dichloromethane
DEPT	Distortionless enhancement by polarization transfer
DIPEA	*N*,*N*-Diisopropylethylamine
DMSO	Dimethyl sulfoxide
DOTA	1,4,7,10-Tetraazacyclododecane-1,4,7,10-tetraacetic acid
DOTA-AHA	1,4,7,10-Tetraazacyclododecane-1-[(6-amino)hexanoic]-4,7,10-triacetic acid
DOTA-A(PEG$_{750}$)HA	1,4,7,10-Tetraazacyclododecane-1-[6-amino(MeO-PEG$_{750}$-succinate)]hexanoic-4,7,10-triacetic acid
DOTA-A(PEG$_{550}$)HA	1,4,7,10-Tetraazacyclododecane-1-[6-amino(MeO-PEG$_{550}$-succinate)]hexanoic-4,7,10-triacetic acid

DOTA-A(PEG$_{350}$)HA	1,4,7,10-Tetraazacyclododecane-1-[6-amino(MeO-PEG$_{350}$-succinate)]hexanoic-4,7,10-triacetic acid
DOTASA	1,4,7,10-Tetraazacyclododecane-1-succinic acid-4,7,10-triacetic acid
ESI	Electrospray ionization
HATU	1-[Bis(dimethylamino)methylene]-1*H*-1,2,3-triazolo[4,5-*b*]pyridinium 3-oxid hexafluorophosphate
HMBC	Heteronuclear multiple bond correlation
HOBt	1-Hydroxybenzotriazole
HOPO	Hetero-tripodal hydroxypyridonate
HSA	Human serum albumin
HSQC	Heteronuclear Single Quantum Coherence
LRMS	Low resolution mass spectrometry
MeCN	Acetonitrile
MRI	Magnetic resonance imaging
NMR	Nuclear magnetic resonance
NMRD	Nuclear magnetic relaxation dispersion
PEG	Poly(ethylene) glycol
SD	Standard deviation
TFA	Trifluoroacetic acid
TMS	Tetramethylsilane
TSP	3-(Trimethylsilyl)propionic-2,2,3,3-d_4 acid sodium salt
TLC	Thin layer chromatography
***t*-Bu**	*tert*-Butyl

Acknowledgements

The authors thank the Foundation for Science and Technology (FCT–Portugal) for financial support through the NMR Portuguese network (Bruker 400 Avance III-Univ Minho); FCT and FEDER (European Fund for Regional Development)-COMPETE/QREN/EU for financial support through the research unity PEst-C/QUI/UI686/2013 and the PhD grant attributed to André Fontes (SFRH/BD/63676/2009) also financed by the POPH and FSE.

Bibliography

[1] S. Mansson, A. Bjornerud, in *The Chemistry of Contrast Agents in Medical Magnetic Resonance Imaging*, John Wiley & Sons, Inc, Chichester, **2001**.

[2] E. Toth, L. Helm, A. A. Merbach, in *The Chemistry of Contrast Agents in Medical Magnetic Resonance Imaging*, John Wiley & Sons, Chichester, **2013**, pp. 25-82.

[3] R. B. Lauffer, *Chem. Rev.* **1987**, *87*, 901-927.

[4] C. F. G. C. Geraldes, S. Laurent, *Contrast Media Mol. Imaging* **2009**, *4*, 1-23.

[5] E. C. Unger, J. D. Schilling, A. N. Awad, K. E. McIntyre, M. T. Yoshino, G. D. Pond, A. Darkazanli, G. C. Hunter, V. M. Bernhard, *JMRI-J. Magn. Reson. Imaging* **1995**, *5*, 1-5.

[6] P. Caravan, J. J. Ellison, T. J. McMurry, R. B. Lauffer, *Chem. Rev.* **1999**, *99*, 2293-2352.

[7] aW.-h. Li, G. Parigi, M. Fragai, C. Luchinat, T. J. Meade, *Inorg. Chem.* **2002**, *41*, 4018-4024; bB. Jebasingh, V. Alexander, *Inorg. Chem.* **2005**, *44*, 9434-9443; cJ. Rudovsky, M. Botta, P. Hermann, A. Koridze, S. Aime, *Dalton Trans.* **2006**, 2323-2333; dY. Song, E. K. Kohlmeir, T. J. Meade, *Journal of the American Chemical Society* **2008**, *130*, 6662-+; eD. J. Mastarone, V. S. R. Harrison, A. L. Eckermann, G. Parigi, C. Luchinat, T. J. Meade, *Journal of the American Chemical Society* **2011**, *133*, 5329-5337; fJ. Tanwar, A. Datta, A. K. Tiwari, S. Chaturvedi, H. Ojha, M. Allard, N. K. Chaudary, M. Thirumal, A. K. Mishra, *Dalton Trans.* **2011**, *40*, 3346-3351.

[8] aE. Toth, I. van Uffelen, L. Helm, A. E. Merbach, D. Ladd, K. Briley-Saebo, K. E. Kellar, *Magn. Reson. Chem.* **1998**, *36*, S125-S134; bB. Zarabi, A. Nan, J. Zhuo, R. Gullapalli, H. Ghandehari, *Mol. Pharm.* **2006**, *3*, 550-557; cH. Y. Lee, H. W. Jee, S. M. Seo, B. K. Kwak, G. Khang, S. H. Cho, *Bioconjugate Chem.* **2006**, *17*, 700-706.

[9] aV. J. Venditto, C. A. S. Regino, M. W. Brechbiel, *Mol. Pharm.* **2005**, *2*, 302-311; bH. Kobayashi, M. W. Brechbiel, *Adv. Drug Deliv. Rev.* **2005**, *57*, 2271-2286; cS. Langereis, A. Dirksen, T. M. Hackeng, M. H. P. van Genderen, E. W. Meijer, *New J. Chem.* **2007**, *31*, 1152-1160.

[10] aJ. P. Andre, E. Toth, H. Fischer, A. Seelig, H. R. Macke, A. E. Merbach, *Chem.-Eur. J.* **1999**, *5*, 2977-2983; bG. M. Nicolle, E. Toth, K. P. Eisenwiener, H. R. Macke, A. E. Merbach, *J. Biol. Inorg. Chem.* **2002**, *7*, 757-769; cW. J. M. Mulder,

G. J. Strijkers, G. A. F. van Tilborg, A. W. Griffioen, K. Nicolay, *NMR Biomed.* **2006**, *19*, 142-164; dA. Fontes, M. I. M. Prata, C. F. G. C. Geraldes, J. P. Andre, *Nuclear Medicine and Biology* **2011**, *38*, 363-370.

[11] aS. Aime, D. D. Castelli, D. Lawson, E. Terreno, *Journal of the American Chemical Society* **2007**, *129*, 2430-2431; bN. Kamaly, T. Kalber, A. Ahmad, M. H. Oliver, P. W. So, A. H. Herlihy, J. D. Bell, M. R. Jorgensen, A. D. Miller, *Bioconjugate Chem.* **2008**, *19*, 118-129; cS. Laurent, L. V. Elst, C. Thirifays, R. N. Muller, *Eur. Biophys. J. Biophys. Lett.* **2008**, *37*, 1007-1014.

[12] J. B. Tang, Y. Q. Sheng, H. J. Hu, Y. Q. Shen, *Prog. Polym. Sci.* **2013**, *38*, 462-502.

[13] J. M. Harris, N. E. Martin, M. Modi, *Clin. Pharmacokinet.* **2001**, *40*, 539-551.

[14] aP. Bailon, A. Palleroni, C. A. Schaffer, C. L. Spence, W. J. Fung, J. E. Porter, G. K. Ehrlich, W. Pan, Z. X. Xu, M. W. Modi, A. Farid, W. Berthold, *Bioconjugate Chem.* **2001**, *12*, 195-202; bA. N. Lukyanov, R. M. Sawant, W. C. Hartner, V. P. Torchilin, *J. Biomater. Sci.-Polym. Ed.* **2004**, *15*, 621-630; cT. Lammers, R. Kuhnlein, M. Kissel, V. Subr, T. Etrych, R. Pola, M. Pechar, K. Ulbrich, G. Storm, P. Huber, P. Peschke, *J. Control. Release* **2005**, *110*, 103-118; dF. M. Veronese, O. Schiavon, G. Pasut, R. Mendichi, L. Andersson, A. Tsirk, J. Ford, G. F. Wu, S. Kneller, J. Davies, R. Duncan, *Bioconjugate Chem.* **2005**, *16*, 775-784.

[15] X. H. He, P. C. Shaw, S. C. Tam, *Life Sci.* **1999**, *65*, 355-368.

[16] aX. Y. Chen, E. Sievers, Y. P. Hou, R. Park, M. Tohme, R. Bart, R. Bremner, J. R. Bading, P. S. Conti, *Neoplasia* **2005**, *7*, 271-279; bA. Vaidya, Y. G. Sun, Y. Feng, L. Emerson, E. K. Jeong, Z. R. Lu, *Pharm. Res.* **2008**, *25*, 2002-2011; cS. J. DeNardo, R. W. Liu, H. Albrecht, A. Natarajan, J. L. Sutcliffe, C. Anderson, L. Peng, R. Ferdani, S. R. Cherry, K. S. Lam, *J. Nucl. Med.* **2009**, *50*, 625-634; dS. H. Hausner, D. L. Kukis, M. K. J. Gagnon, C. E. Stanecki, R. Ferdani, J. F. Marshall, C. J. Anderson, J. L. Sutcliffe, *Mol. Imaging* **2009**, *8*, 111-121; eL. Li, F. Turatti, D. Crow, J. R. Bading, A. L. Anderson, E. Poku, P. J. Yazaki, L. E. Williams, D. Tamvakis, P. Sanders, D. Leong, A. Raubitschek, P. J. Hudsony, D. Colcher, J. E. Shively, *J. Nucl. Med.* **2010**, *51*, 1139-1146; fS. Dapp, C. Muller, E. G. Garayoa, P. Blauenstein, V. Maes, L. Brans, D. A. Tourwe, R. Schibli, *EJNMMI research* **2012**, *2*, 24; gJ. Gallo, I. S. Alam, J. Jin, Y.-J. Gu, E. O. Aboagye, W.-T. Wong, N. J. Long, *Dalton Trans.* **2014**, *43*, 5535-5545.

[17] aD. M. J. Doble, M. Botta, J. Wang, S. Aime, A. Barge, K. N. Raymond, *Journal of the American Chemical Society* **2001**, *123*, 10758-10759; bM. Botta, S. Quici, G. Pozzi, G. Marzanni, R. Pagliarin, S. Barra, S. G. Crich, *Org. Biomol. Chem.* **2004**, *2*, 570-577; cM. K. Thompson, D. M. J. Doble, L. S. Tso, S. Barra, M. Botta, S. Aime, K. N. Raymond, *Inorg. Chem.* **2004**, *43*, 8577-8586.

[18] aE. C. Unger, D. K. Shen, G. L. Wu, L. Stewart, T. O. Matsunaga, T. P. Trouard, *Magn. Reson. Mat. Phys. Biol. Med.* **1999**, *8*, 154-162; bP. Mi, H. Cabral, D. Kokuryo, M. Rafi, Y. Terada, I. Aoki, T. Saga, I. Takehiko, N. Nishiyama, K. Kataoka, *Biomaterials* **2013**, *34*, 492-500.

[19] aL. D. Margerum, B. K. Campion, M. Koo, N. Shargill, J. J. Lai, A. Marumoto, P. C. Sontum, *J. Alloy. Compd.* **1997**, *249*, 185-190; bH. Kobayashi, S. Kawamoto, T. Saga, N. Sato, A. Hiraga, T. Ishimori, J. Konishi, K. Togashi, M. W. Brechbiel, *Magn.Reson.Med.* **2001**, *46*, 781-788; cZ. Jaszberenyi, L. Moriggi, P. Schmidt, C. Weidensteiner, R. Kneuer, A. E. Merbach, L. Helm, E. Toth, *J. Biol. Inorg. Chem.* **2007**, *12*, 406-420.

[20] A. Fontes, S. Karimi, L. Helm, M. Yulikov, P. M. Ferreira, J. P. André, *Eur. J. Inorg. Chem.* **2015**, *2015*, 1579-1591.

[21] S. Laurent, L. V. Elst, R. N. Muller, *Contrast Media Mol. Imaging* **2006**, *1*, 128-137.

[22] aF. A. Dunand, E. Toth, R. Hollister, A. E. Merbach, *J. Biol. Inorg. Chem.* **2001**, *6*, 247-255; bF. Yerly, A. Borel, L. Helm, A. E. Merbach, *Chemistry – A European Journal* **2003**, *9*, 5468-5480.

[23] aJ. A. Peters, E. Zitha-Bovens, E. Corsi, C. F. G. C. Geraldes, in *The Chemistry of Contrast Agents in Medical Magnetic Resonance Imaging* (Eds.: E. Toth, A. E. Merbach), Wiley, Chichester, **2001**; bL. Frullano, J. Rohovec, J. A. Peters, C. Geraldes, in *Contrast Agents I: Magnetic Resonance Imaging, Vol. 221* (Ed.: W. Krause), Springer-Verlag Berlin, Berlin, **2002**, pp. 25-60; cS. Aime, M. Botta, M. Fasano, M. P. M. Marques, C. F. G. C. Geraldes, D. Pubanz, A. E. Merbach, *Inorg. Chem.* **1997**, *36*, 2059-2068.

[24] S. Aime, M. Botta, E. Garino, S. G. Crich, G. Giovenzana, R. Pagliarin, G. Palmisano, M. Sisti, *Chem.-Eur. J.* **2000**, *6*, 2609-2617.

[25] aJ. F. Desreux, *Inorg. Chem.* **1980**, *19*, 1319-1324; bS. Aime, M. Botta, G. Ermondi, *Inorg. Chem.* **1992**, *31*, 4291-4299; cV. Jacques, J. F. Desreux, *Inorg. Chem.* **1994**, *33*, 4048-4053; dM. P. M. Marques, C. F. G. C. Geraldes, A. D.

Sherry, A. E. Merbach, H. Powell, D. Pubanz, S. Aime, M. Botta, *J. Alloy. Compd.* **1995**, *225*, 303-307.

[26] J. P. Andre, E. Brucher, R. Kiraly, R. A. Carvalho, H. Macke, C. Geraldes, *Helvetica Chimica Acta* **2005**, *88*, 633-646.

[27] aJ. Rudovský, P. Cígler, J. Kotek, P. Hermann, P. Vojtíšek, I. Lukeš, J. A. Peters, L. Vander Elst, R. N. Muller, *Chemistry – A European Journal* **2005**, *11*, 2373-2384; bC. Platas-Iglesias, *Eur. J. Inorg. Chem.* **2012**, *2012*, 2023-2033.

[28] aJ. A. K. Howard, A. M. Kenwright, J. M. Moloney, D. Parker, M. Port, M. Navet, O. Rousseau, M. Woods, *Chem. Commun.* **1998**, 1381-1382; bM. Woods, S. Aime, M. Botta, J. A. K. Howard, J. M. Moloney, M. Navet, D. Parker, M. Port, O. Rousseaux, *Journal of the American Chemical Society* **2000**, *122*, 9781-9792; cS. Aime, M. Botta, G. Ermondi, E. Terreno, P. L. Anelli, F. Fedeli, F. Uggeri, *Inorg. Chem.* **1996**, *35*, 2726-2736.

[29] E. Toth, L. Helm, A. A. Merbach, in *The Chemistry of Contrast Agents in Medical Magnetic Resonance Imaging*, John Wiley & Sons, Chichester, **2013**, pp. 209-276.

[30] aS. Aime, A. Barge, M. Botta, A. S. De Sousa, D. Parker, *Angew. Chem.-Int. Edit.* **1998**, *37*, 2673-2675; bS. Aime, A. Barge, J. I. Bruce, M. Botta, J. A. K. Howard, J. M. Moloney, D. Parker, A. S. de Sousa, M. Woods, *Journal of the American Chemical Society* **1999**, *121*, 5762-5771; cF. A. Dunand, S. Aime, A. E. Merbach, *Journal of the American Chemical Society* **2000**, *122*, 1506-1512.

[31] J. P. Andre, H. R. Maecke, E. Toth, A. A. Merbach, *J. Biol. Inorg. Chem.* **1999**, *4*, 341-347.

[32] H. E. Gottlieb, V. Kotlyar, A. Nudelman, *J. Org. Chem.* **1997**, *62*, 7512-7515.

[33] C. Ammann, P. Meier, A. E. Merbach, *J. Magn. Reson.* **1982**, *46*, 319-321.

[34] G. Brunisholz, M. Randin, *Helvetica Chimica Acta* **1959**, *42*, 1927-1938.

[35] D. M. Corsi, C. Platas-Iglesias, H. v. Bekkum, J. A. Peters, *Magn. Reson. Chem.* **2001**, *39*, 723-726.

[36] aA. D. Hugi, L. Helm, A. E. Merbach, *Helvetica Chimica Acta* **1985**, *68*, 508-521; bI. Solomon, *Physical Review* **1955**, *99*, 559-565.

[37] R. L. Vold, J. S. Waugh, M. P. Klein, D. E. Phelps, *The Journal of Chemical Physics* **1968**, *48*, 3831-3832.

[38] S. Meiboom, D. Gill, *Review of Scientific Instruments* **1958**, *29*, 688-691.

[39] aN. Bloembergen, *The Journal of Chemical Physics* **1957**, *27*, 572-573; bN. Bloembergen, L. O. Morgan, *The Journal of Chemical Physics* **1961**, *34*, 842-850.

[40] aG. Lipari, A. Szabo, *Journal of the American Chemical Society* **1982**, *104*, 4546-4559; bG. Lipari, A. Szabo, *Journal of the American Chemical Society* **1982**, *104*, 4559-4570.

[41] F. Yerly, EPFL, Lausanne, **2003**.